

We are IntechOpen, the world's leading publisher of Open Access books Built by scientists, for scientists

6,900

Open access books available

186,000

International authors and editors

200M

Downloads

Our authors are among the

154

Countries delivered to

TOP 1%

most cited scientists

12.2%

Contributors from top 500 universities



WEB OF SCIENCE™

Selection of our books indexed in the Book Citation Index
in Web of Science™ Core Collection (BKCI)

Interested in publishing with us?
Contact book.department@intechopen.com

Numbers displayed above are based on latest data collected.
For more information visit www.intechopen.com



EMC Measurement Setup Based on Near-Field Multiprobe System

*Rubén Tena Sánchez, Lars Jacob Foged
and Manuel Sierra Castañer*

Abstract

Multiprobe spherical near-field measurement is a potent tool for fast and accurate characterization of electrical properties of antennas. The use of fast switching in one axis, an azimuth positioner, and a near- to far-field transformation allows a substantial time reduction in antenna measurements while maintaining high-quality results. On the other hand, conventional emissions EMC measurement systems are typically based on detecting the radiated spurious emissions by a device at different frequencies. The systems usually work in far-field (or quasi-far-field conditions), performing the measurements either at 3 or 10 meters. Measurements under these conditions take space and time. Moreover, the systems are not cost-effective for pre-compliance purposes where pre-testing of the device should provide valuable information and confidence about the DUT before performing a compliance test. This chapter analyzes the possibility of cost and space reduction for EMC systems based on multiprobe near-field measurement systems in combination with OTA (over the air measurements), reference-less systems, spherical near-field transformation, phase reconstruction, modal filtering, source reconstruction, and software-defined radio receivers.

Keywords: electromagnetic compatibility, measurements, near-field, multiprobe, over-the-air

1. Introduction

Electromagnetic Compatibility systems are well established and have been widely studied during the last decades. There are a lot of references in this area, like [1]. On the other hand, multiprobe spherical near-field measurements systems have been extensively used for antenna characterization, becoming a potent tool for fast and accurate characterization of electrical properties of antennas. The use of fast switching in one axis, an azimuth positioner, and a near- to far-field transformation allows a substantial time reduction in antenna measurements while maintaining high-quality results. During the last years, combining these kinds of tools with post-processing techniques to increase the accuracy of the measurements and reduce some spurious effects like noise, leakage or echoes, has shown promising results [2]. As explained in the same book, the combination of measurements with simulations has shown the possibility of considering some effects of the measurement scenario.

On the other hand, conventional EMC systems are typically based on detecting the maximum power radiated by a device at different frequencies. The systems

usually work in far-field (or quasi-far-field conditions), performing the measurements either at 3 or 10 meters, but sometimes the device's position under test (DUT) in the setup affects the measurement. Even if there are very well-established standards for EMC measurements to get these peak values and check good performance (low radiation) of the electronic devices, the measurement uncertainty is higher than the one found for antenna measurements.

Some practical radiation emission measurement solutions try to overcome the high cost of pre-compliance chambers that typically can go up to hundreds of thousands of euros. These solutions are based on small systems implemented by robotic arms to scan the volume around the DUT [3–7]. The solution is well suited for diagnostics since the field can be measured very close to the DUT. Moreover, the low-cost systems typically are not shielded, and the phase recovery capabilities are strongly setup dependent. Nevertheless, just a few of them are able to reconstruct the phase and thus compute the field at 3 or 10 meters from the near-field information.

This chapter analyzes the possibility of cost and space reduction for radiation emission EMC measurement systems based on the use of techniques already used in near-field antenna measurements, including near to far-field transformation algorithms, OTA (over the air measurements), reference-less systems, multiprobe arrays, phase reconstruction, modal filtering, source reconstruction, and software-defined radio receivers. During the last years, the authors have been working on all those topics for the complete EMC system, as can be observed in different papers in journals and conferences [8–13], and this chapter summarizes all the work included in those previous research works. The chapter describes the advantages of low-cost near-field measurement systems that could be used for EMC pre-compliance measurements, showing some practical results.

The following sections will focus on several of the essential aspects of this kind of system. Section 2 will explain the possible near-field EMC system architectures, explaining each subsystem (hardware or software). Section 3 will explain the configuration of multiprobe array systems for over-the-air (OTA) systems. Section 4 will explain the amplitude and phase calculation using cheap and integrated Software Defined Radio (SDR) receivers. Section 5 will focus on the effects of near to far-field spherical transformation algorithms, and Section 6 will introduce some of the post-processing techniques that can be included for EMC systems. As the reader can observe, all these techniques have been widely used in antenna measurements, although there is still an open research line to redefine their limitations for EMC measurements, where the objective is to detect the radiated power peak values instead of the 3D radiation pattern.

2. EMC system architecture

The near-field EMC measurement system proposed is based on the architecture of a multiprobe near-field antenna measurement system. In this case, we are using some of the conventional Microwave Vision Group measurement multiprobe setups [14]. These systems are based on wideband dual-polarized probes located on arch systems. The receiver is switching between probe and probe in order to acquire the amplitude and phase of the electromagnetic field generated by the probe. Instead of using a conventional vector network analyzer, in this case, we have replaced the receiver with an SDR platform, whose performance will be shown in the following section. For this application, the DUT is self-transmitting, and, therefore, it is not necessary to include a specific transmitter, or in that case, the transmitter is not synchronized with the receiver, as in the conventional antenna measurement

systems. This is called over-the-air (OTA) systems, although the procedure we use for this specific application is called reference-less system [11, 12] since the reference is not extracted from the transmitter but from a fixed probe.

Two different architectures that can be used for phase reconstruction in a multiprobe system are presented. The first one is based on an external fixed probe whose relative position is kept fixed with respect to the DUT (**Figure 1**). In this case, the reference antenna is sensitive to amplitude and phase changes (proximity to mast, motor, cable, and multiple reflections). Nevertheless, it will be seen that excellent performance can be achieved with such a simple setup while keeping the advantages of a multiprobe system. Moreover, the solution is scalable and could be implemented in multiprobe systems of different sizes to cover larger DUTs or lower frequencies.

The second solution is based on a reference channel for phase reconstruction that uses one of the probes of the multiprobe arch. This solution does not need any additional hardware, but the complexity is transferred to the post-processing techniques. The solution is described in **Figure 2**. In this case, the setup is simplified, and the coupling between probes reduced since the reference channel belongs to the multiprobe arch.

Some extra post-processing steps are needed in order to retrieve the phase information [11]. The results obtained with this setup can be better than using an external reference antenna; nevertheless, the complexity arises for situations in which the elevation arch needs to be rotated. In this case, the top-probe is not on-axis, and further mathematical derivations are needed in order to reconstruct the near-field phase. This can be done by a non-convex iterative optimization algorithm, as explained in [15].

The next step is the near to near-to-far-field transformation. The theory included in [16], proposed by Prof. Hansen in 1973, and widely used in antenna

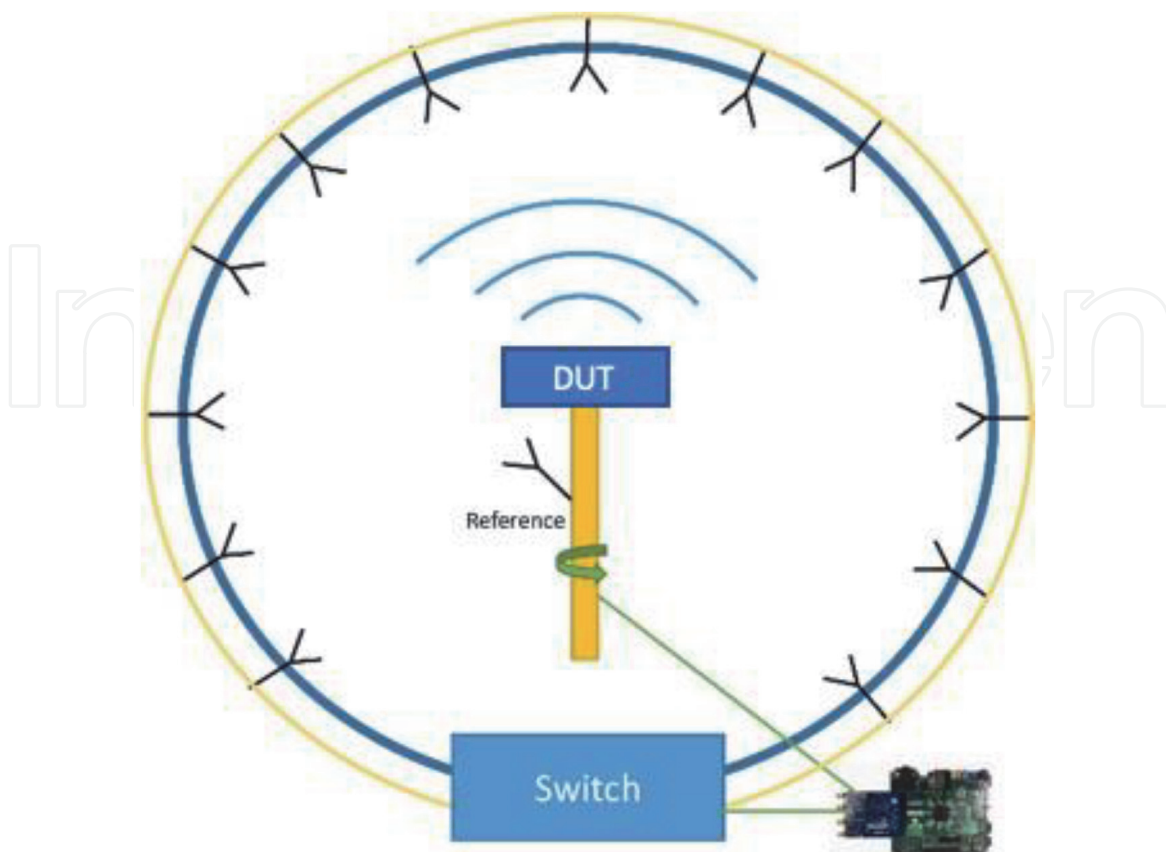


Figure 1.
Measurement setup based on external reference antenna.

near-field measurement is used. This theory is based on the decomposition of the electromagnetic field in spherical mode coefficients, using as input information the amplitude and phase of both orthogonal tangential electric field components (theta and phi) in a sphere enclosing the DUT. Once the spherical mode coefficients are calculated, the field can be computed at any desired distance, in particular 3 or 10 meters.

Some post-processing techniques appeared during the last year that use the information available of the antenna under test and the measurement system, could also be used to improve the results of these EMC measurements. These techniques are based on the filtering of the electromagnetic field in other domains: time domain, antenna electromagnetic sources, spherical modes, or cylindrical modes. A summary of all these techniques can be found in [2], and some of them have been used for extracting the results presented in this work.

Finally, the results are compared with the conventional EMC standards [17, 18] for the different cases to ensure that the DUT passes the final compliance testing in terms of radiation. In comparison with other compact and low-cost solutions, the use of a shielded and anechoic environment that is typically used for antenna characterization [14] provides accurate results when calculating the radiated field at a finite distance. For source reconstruction, the solution proposed here is based on the commercial software INSIGHT [19]. The measured tangential components of the near-field can be exported, and the equivalent currents of the DUT

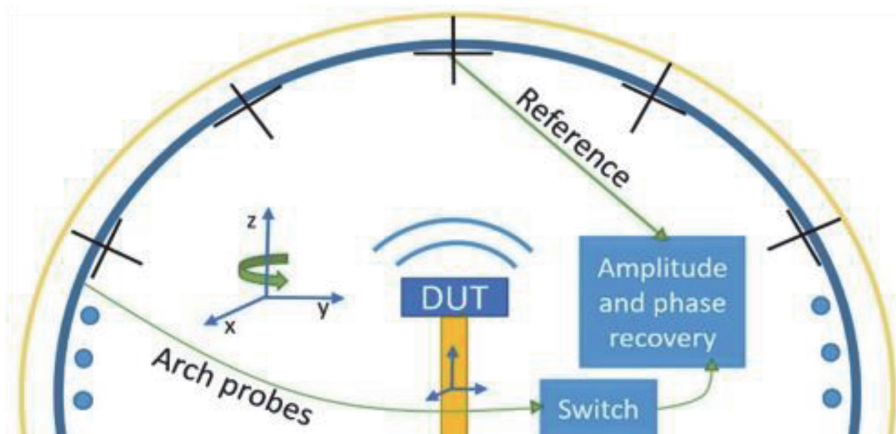


Figure 2.
Measurement setup based on the top probe as a reference antenna.

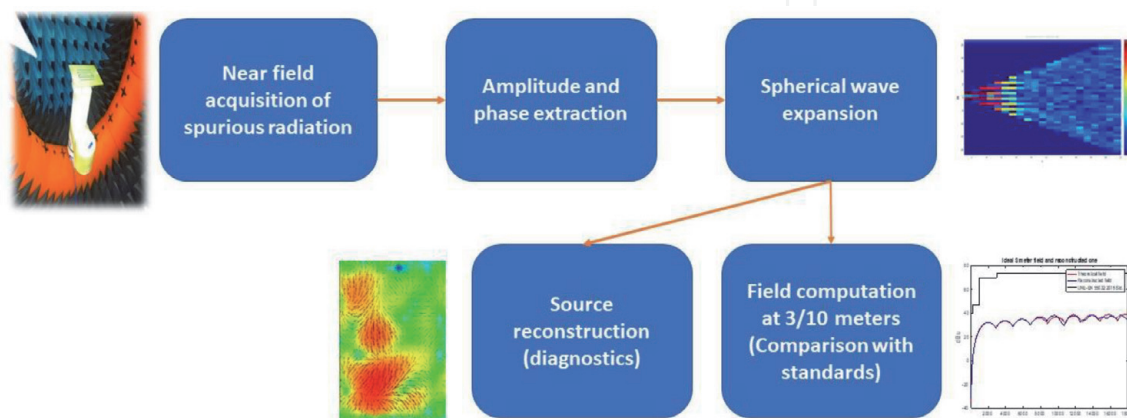


Figure 3.
EMC spurious emissions characterization with near-field multiprobe solutions.

reconstructed in order to determine which areas of the DUT might be responsible for the non-desired radiated emissions.

Figure 3 summarizes the process, and in the following sections, the different parts will be explained.

3. The configuration for multiprobe array systems as OTA system

The hardware of the EMC near-field measurement solution is based on multiprobe systems in combination with the acquisition through a low-cost receiver. The system is based on an arch where the different wideband dual-polarized probes are located. For this specific work, two systems are used: StarLab [20] and MiniLab [21]. These two systems are compact and allow a faster design process and shorter time to market times while keeping a reasonable cost. The use of the low-cost receiver reduces the complexity drastically and cost in comparison with traditional spectrum or vector network analyzers. Moreover, the systems are scalable; thus, the size or low-frequency limitation can be overcome by increasing the measurement solution using other multiprobe configurations.

Figure 4 shows both systems: MiniLab is the smallest system and works from 650 MHz up to 6 GHz. The radius of the arch is 30 cm with 12 dual linear polarized probes separated by fixed angular steps of 15 degrees. The maximum size of the device under test is 40 cm. StarLab can work from 650 MHz up to 18 GHz for a maximum size of DUT of 45 cm, with up to 15 probes (depending on the model and frequency band). In this case, the system allows a rotation of the arch to increase the number of samples in elevation. In both cases, the use of special receivers allows the working in an over-the-air mode, useful for EMC, 5G, IoT, MIMO, and other special measurement systems. A system calibration process is necessary to assure a reasonable calculation of amplitude, polarization, and phase in the multiprobe system.

In all these systems, the receiver is switching among the different probes, and the amplitude and phase of both polarizations are acquired. One antenna is used as a reference to extract the relative phase among the different probes. As it was already stated before, there are two ways to extract the phase: either by using the on-axis probe of the multiprobe system or by displacing another reference antenna. In the second case, the coupling with the system can be more significant, but still, acceptable results can be achieved [9, 10].



Figure 4. Microwave vision group minilab (left) and StarLab (right).

4. Amplitude and phase extraction using SDR receivers

The low-cost reference-less receiver is implemented using the Zynq Evaluation and Development Board (Zed- Board) with the transceiver AD-FMCOMMS3- EBZ. This RF transceiver includes a configurable digital interface to an FPGA to communicate the ZedBoard and the RF module. The 2x2 transceiver module consists of a 12-bit ADC with a receiver band from 70 MHz to 6 GHz and a tunable channel bandwidth up to 56 MHz. This receiver is homodyne, and the signal is directly down-converted to base-band for digitization purposes. The I-Q samples are generated by the transceiver module. The receiver chain can be externally controlled, and it consists of two programmable low-pass filters, decimating filters and gains control for each channel.

The receiver is based on time-domain measurements. Then, the amplitude extraction is done by means of frequency-domain techniques. The power calculation is based on Parseval's theorem on the discrete-time form, see Eq. (1). In the equation, $X(k)$ refers to the Fourier basis functions, while $x(n)$ represents the sampled time-domain signal received by the probe. The number of samples N plays an important role if noise averaging is implemented. Post-processing steps like windowing and filtering are applied in order to get accurate results, see [12].

$$\frac{1}{N} \sum_{n=0}^{N-1} |x(n)|^2 = \frac{1}{N^2} \sum_{k=0}^{N-1} |X(k)|^2 \quad (1)$$

Phase reconstruction is not that straightforward, and the method depends on the system architecture: reference antenna independent from measurement arch or on-axis reference antenna. For this application, the transmitters are not necessary.

4.1 Phase extraction for reference antenna independent from measurement arch

If the reference antenna is displaced around the AUT in a fixed relative position, the reference channel emulates the conventional sample taken from a vector network analyzer. In that case, the relative phase between measurement points of the DUT can be extracted as described by Eq. (2). The value of k_1 determines the intermediate frequency of the computation.

$$\phi_i = \arg \left\{ \frac{\sum_{n=0}^{N-1} E_{\text{multiprobe}}(n) e^{-j\frac{2\pi}{N} k_1 n}}{\sum_{n=0}^{N-1} E_{\text{reference}}(n) e^{-j\frac{2\pi}{N} k_1 n}} \right\} \quad (2)$$

This method considers possible drifts in the transmitted signal of the DUT since the reference sample is taken by radiation. In contrast with other existing solutions for phase retrieval that could be used for EMC measurements, this one exploits the intrinsic advantages of multiprobe solutions that allow for better isolation of the reference antenna while providing an anechoic and shielded measurement environment. Besides, the reference is accurate as long as the interference from the reference antenna is kept small. This method has already been applied for planar as well as for spherical multiprobe measurements by the authors [12].

4.2 Phase extraction for on-axis reference antenna from multiprobe measurement arch

When the reference antenna belongs to the measurement arch, the solution is simplified. In comparison with the external reference antenna solution, there are some substantial changes:

- The multiprobe system is composed of dual-polarized probes at each sample point. The phase reference will be obtained by taking as reference only one polarization, which means that all the measured phases are relative phases with respect to the reference probe for that polarization.
- When the system rotates to measure the whole sphere, there is a change in the reference on-axis probe signal. Therefore, the relative phases for each cut are referenced to one of the top probe polarization when it is rotated.

The change in the phase reference is translated into phase unknowns for every azimuthal cut, as described by Eq. (3). These unknowns are solved by appealing to Ludwig's III definition of polarization that allows retrieving the phase unknowns of the measured signals in a direct way, as explained in [15].

$$\begin{aligned}\vec{E}_{meas}(\phi_1) &= \vec{E}_{ref} \\ \vec{E}_{meas}(\phi_2) &= \vec{E}(\phi_2)e^{j\phi_2} \\ &\vdots \\ \vec{E}_{meas}(\phi_N) &= \vec{E}(\phi_N)e^{j\phi_N}\end{aligned}\quad (3)$$

5. Near to far-field spherical transformation algorithm for EMC

Every receiving probe measures the field radiated by the DUT. The well-known transmission formula [16] gives the relation between the signal measured by the probe and the spherical modes coefficients:

$$w(r, \chi, \theta, \varphi) = \sum_{smn\mu} Q_{smn} e^{jm\varphi} d_{\mu m}^n(\theta) e^{j\mu\chi} P_{s\mu n}(r) \quad (4)$$

being (r, θ, φ) spherical coordinates, χ the probe orientation, Q_{smn} the AUT spherical wave coefficients, $d_{\mu m}^n(\theta)$ a rotation operator and $P_{s\mu n}(r)$ the probe response constants. The summation in Eq. (4) spans for $s \in [1, 2]$, $n \in [1, N]$, $m \in [-n, n]$ and $\mu \in [-V, V]$. N and V are the expansion truncation numbers for the AUT and antenna probe, respectively. In principle, this number is infinite. However, depending on the antenna, the number of SWC with significant power is finite for both AUT and probe, and there exists the following practical rule for maintaining good accuracy:

$$N = \lceil kr_0 \rceil + 10 \quad (5)$$

where k is the wavenumber, r_0 the radius of the smallest sphere circumscribing the AUT (or probe in the case of V), and the brackets indicate the largest integer smaller than or equal to the number inside them. However, this rule of Eq. (5) can be replaced by more complicated expressions depending on the signal to noise [22]. For a mode power of 40 dB below the maximum, a more accurate expression is shown in Eq. (6).

$$N = \lceil kr_0 \rceil + 1.6\sqrt[3]{kr_0} \quad (6)$$

Once the spherical modes are calculated, the field generated by the probe can be calculated for each specific point at a finite or infinite distance.

A representative example of the spherical wave expansion of an EMC device can be simulated by taking as DUT a 15 cm dipole excited with 1 μ A current. The field

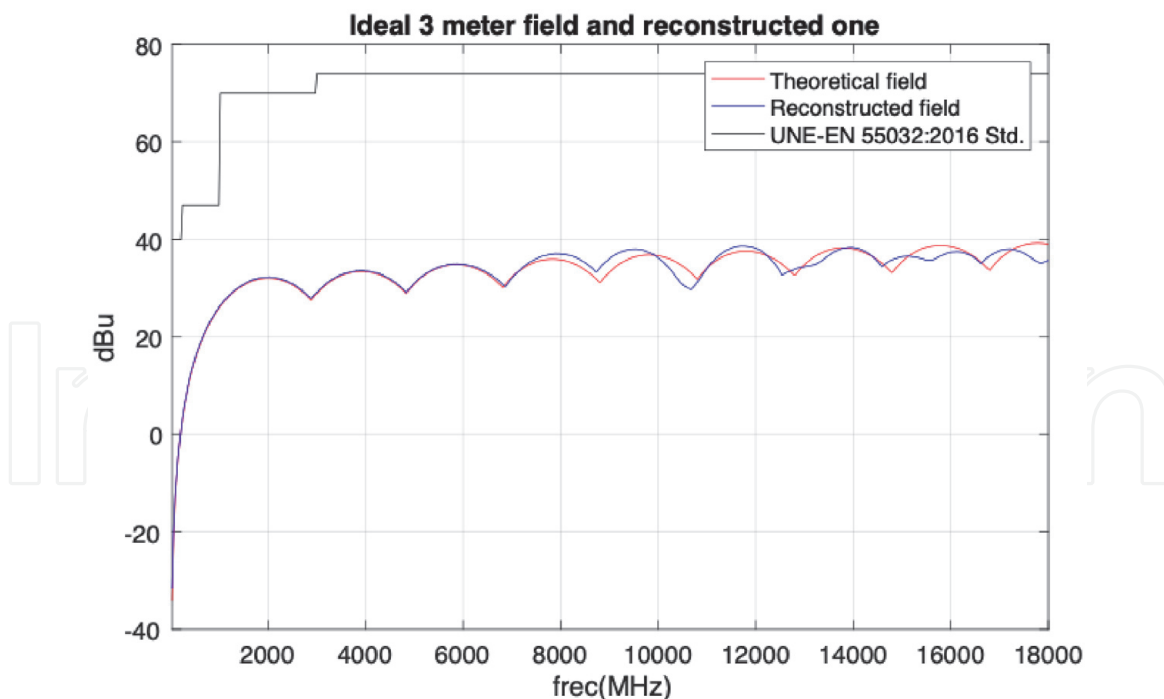


Figure 5.
Comparison of analytical electromagnetic field and field after the spherical transformation process to 3 m.

generated at 3 meters is analytically calculated and compared with the one obtained by following the near-field acquisition by an EMC multiprobe system. In this case, the probes are modeled with antenna factors of 0.1 (to represent a poor performance), the receiver includes a Gaussian noise equal to -120 dBm (the one of the SDR platform), and 12 dual linear polarized probes separated 15 degrees at a radial distance of 30 cm are considered, to emulate the MiniLab multiprobe system.

Figure 5 shows the results for the peak values, comparing them with the UNE-EN 55032:2016 Std. [18]. The standard level is included to show that the process has the required low power to ensure that the noise effect is negligible. For low frequencies, a spherical mode truncation is applied to run the transformation algorithm without numerical problems. In higher frequencies, the differences are due to undersampling effects: this is due to the limited number of samples, 15 degrees separation between probes, compared with the dimension of the device under test and higher frequencies. However, up to 6 GHz, the system works very well. For frequencies up to 18 GHz, the solution is to implement the arch rotation and use a non-convex optimization for phase retrieval [15].

6. Practical implementation of radiated spurious near-field multiprobe measurement system

To validate the system for radiated EMC measurements, two experiments have been performed. In those experiments, different post-processing techniques are used to improve the results. The same reference DUT sample is used in both cases: this consists of a PCB of 150 mm by 225 mm with a substrate thickness of 2 mm. One of the traces of the PCB is excited through an external transmitter, while the other ones are excited through coupling. The DUT represents a bad radiator, so it is a good sample of a typical EMC device.

The first experiment was done in MVG Italy by using StarLab in one of the possible EMC configurations: a reference antenna independent from the arch and SDR receiver. The DUT was also measured in a certified laboratory. In particular,

the DUT was measured in CATECHOM [23] (University of Alcalá, Spain). According to the technical specifications marked by the European Standards (EN), the laboratory is certified to perform EMC measurements, providing the certification process required for the CE mark of a product. A comparison of both configurations can be seen in **Figure 6**.

The characteristics of each measurement solution are described in **Table 1**. The main difference is the measurement time, which can be drastically reduced with the multiprobe EMC solution while keeping a good accuracy, as will be seen. The processing time for the NF transformation to 3/10 meters distance is negligible.

In order to measure the multiprobe EMC system, an electric sleeve dipole was used as a reference antenna. Three different signals are compared: as a reference, the measurement in the conventional multiprobe configuration of Starlab (45 cm distance), using the vector network analyzer to feed the DUT and thus, having access to the reference signal to measure the amplitude and phase. Then, the multiprobe EMC configuration measurement is performed, where the reference antenna does the phase retrieval, and the SDR is used to reconstruct the amplitude and phase near-field pattern. Finally, the conventional EMC laboratory (CATECHOM) measurement at a 3 meters distance is done. The flowchart of the comparison procedure and post-processing steps are shown in **Figure 7**.

The results herein presented correspond to 2 GHz. In the flowchart, CST [24] was used before performing the final comparison. This was necessary to include the effect of the wooden table in the device's radiation when measured in the certified EMC laboratory. This is also an added value of the multiprobe EMC solution since the radiated emission can be computed, including different scatterers around the DUT. Moreover, source reconstruction was done by using Insight [19]. This source reconstruction is able to calculate the currents on the PCB structure, filtering out all the contributions out of the PCB itself. As shown in [2], this technique can improve the results of the measurements. This allows comparing how accurate the EMC multiprobe solution could be compared to the ideal source reconstruction that can be achieved with the vector network analyzer measurements.

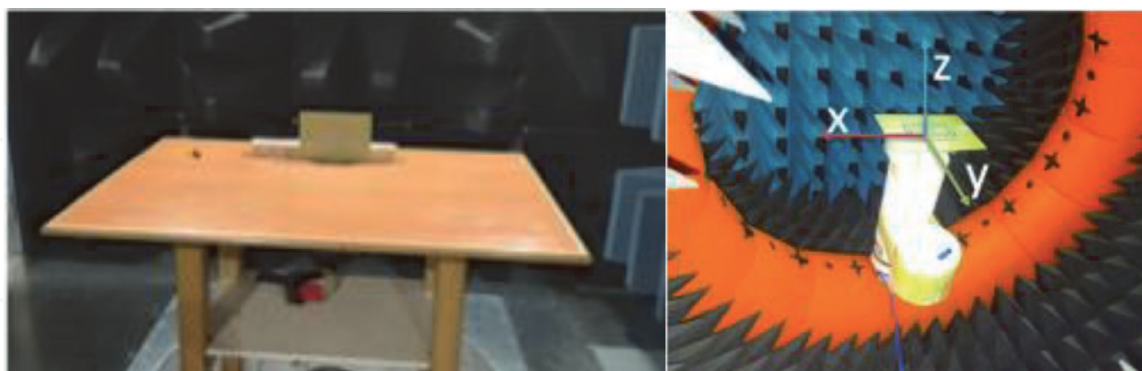


Figure 6.
 EMC test-case: Compliance laboratory (CATECHOM), and multiprobe EMC system.

Measurement system	Measurement distance	Geometry	Measurement time
CATECHOM	3 m	Height variation and azimuth sweep	≈3 hours
EMC Multiprobe	45 cm (NF to NF/FF transformation)	Azimuth rotation, multiprobe in elevation	≈10 min

Table 1.
 Measurement characteristics: Conventional EMC measurement and multiprobe EMC solution.

The radiation pattern results at 3 m are shown in **Figure 8**. In this case, from the near-field, the sources are reconstructed, and once these currents are calculated, the electromagnetic field at 3 meters is calculated using the commercial software CST for both horizontal and vertical polarizations. It was done in this way to consider the table used to support the PCB. The results show that the difference between using a conventional VNA (most accurate system) and the SDR platform is minimal. This opens the possibility of low-cost receivers for this kind of system. Second, the differences with respect to the measurements with a conventional EMC setup are within the uncertainty of these systems. The main advantages of using near-field systems are the lower uncertainty in the measurement process, due to the easier control of the environment, and the possibility of including some external setups, using commercial electromagnetic software such as CST.

Nevertheless, the peak error for the maximum of the radiation is below 2 dBV/m. The comparison of the pattern is suggesting that the angular variation of the radiated emission is appropriately reconstructed. This would be translated into a good correlation of the currents' distribution. The source reconstruction comparison between the measurements done with the vector network analyzer and the multiprobe EMC setup can be seen in **Figure 9**.

Another experiment was performed in the MiniLab system of Microwave Vision Group in Pomezia (Italy). This system was used in a different architecture for EMC multiprobe solutions (**Figure 2**), with the on-axis top-probe used as a reference channel. In order to measure with this architecture, hardware modifications are needed since one of the connected signals to the conventional switching matrix of a multiprobe system is connected to one input of the SDR receiver. Thereby, a

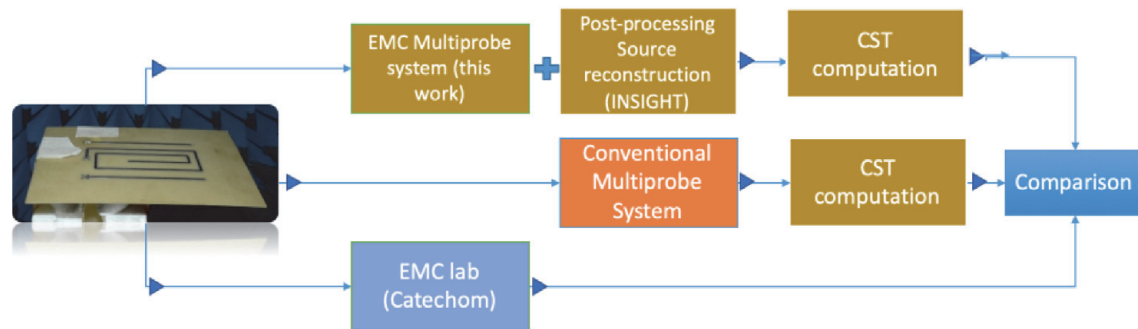


Figure 7.
Process for comparison of the measurements of the PCB structure.

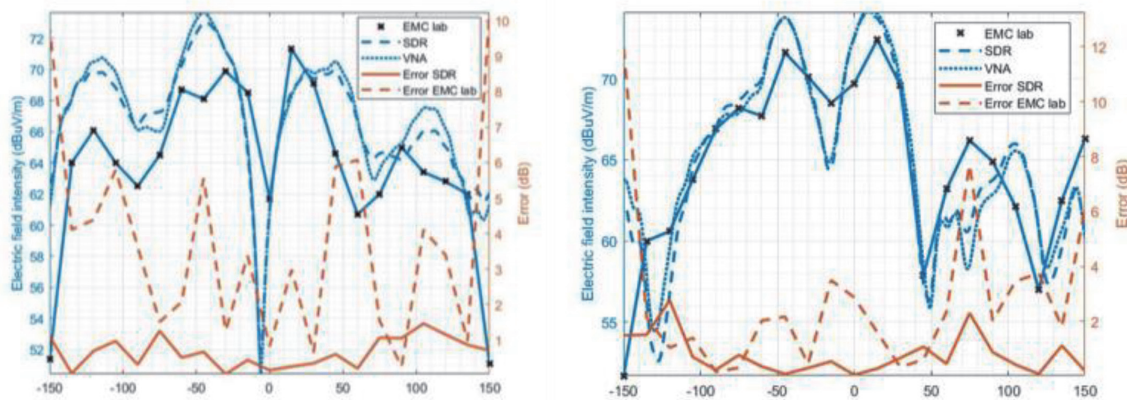


Figure 8.
Comparison between conventional measurement and measurement using near-field procedure: With conventional VNA and SDR platform (H component left and V component right).

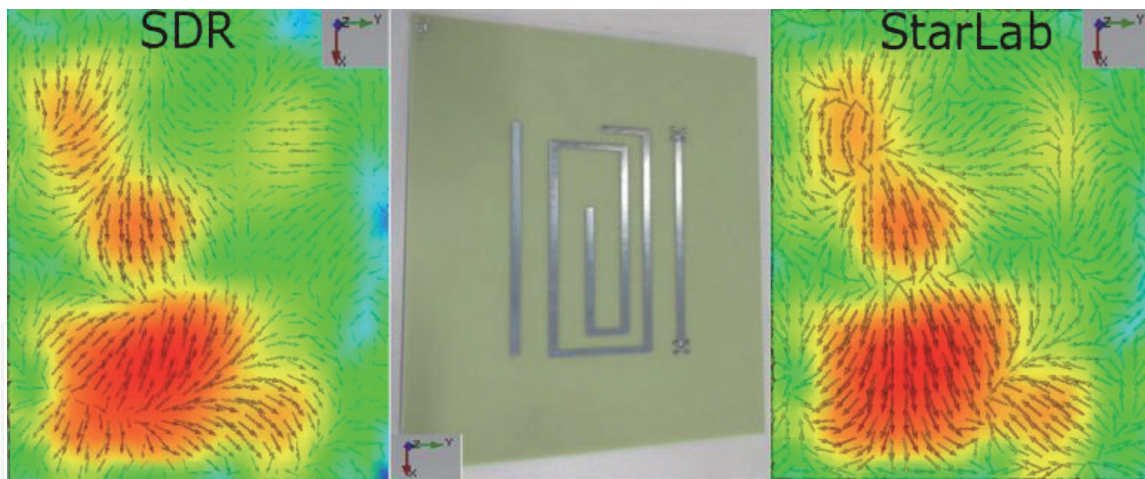


Figure 9.
Source reconstruction on top of DUT.

calibration is needed in order to account for differences between the switching matrix RF path and the direct connection of the on-axis probe.

The goal of the experiments was to verify the performance of the multiprobe EMC solution based on the on-axis probe as a reference when it comes to modulated EMC signals. Some other experiments were performed with continuous-wave signals to validate the system. As was the case for the antenna independent from the measurement arch, good results were obtained, and some results can be found in [11].

It is well known that some DUTs could work with modulated signals. The extrapolation of radiation parameters for modulated signals and how to measure them is not that clear [25]. Some experiments have been done in order to validate EMC multiprobe measurements of modulated signals. In that sense, let us assume there is an IoT device transmitting a modulated signal. Let us also assume that the signal is LTE FDD type. Emulation of this scenario was done by exciting a known antenna with a modulated LTE FDD signal of a predefined bandwidth (see **Figure 10**).

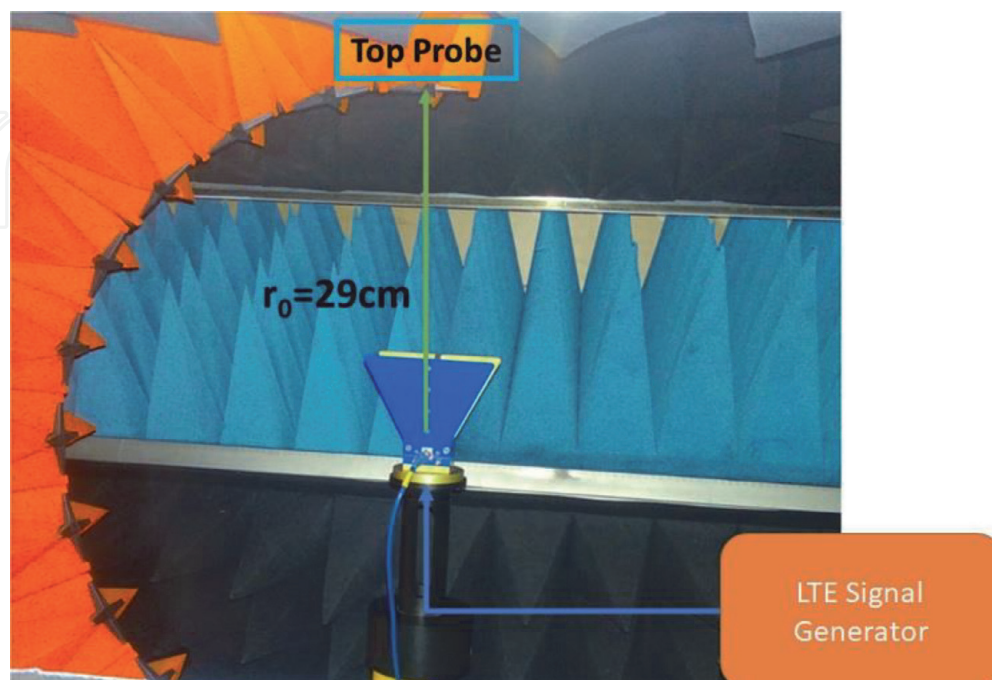


Figure 10.
On-Axis architecture of multiprobe EMC system for LTE measurements.

The SDR was optimized in order to extract the time domain near-field amplitude and phase of the transmitted signal. In the particular case of the results herein presented, an LTE FDD signal of 5 MHz bandwidth is analyzed. The parameters extraction is done in a similar way it is done for a continuous wave signal. For the power, the spectrum under interest is integrated. For the phase, linearity is assumed in such a way that the average (intermediate) phase over the whole bandwidth represents, ideally, the radiation pattern of the DUT at the central frequency. This statement is mathematically described by Eq. (7). In the equation, the measured phase at equispaced frequencies from the central one (f_c) cancels out, giving the measured phase at the central frequency as a result. This is true under the assumption that the radiation pattern of the DUT is not changing over the given bandwidth, which is true for most practical cases.

$$\frac{1}{N+1} \sum_{i=-N/2}^{N/2} \phi_{meas}(f_c + i\Delta_f) = \phi_{meas}\left(f_c - \frac{N}{2}\Delta_f\right) + \dots + \phi_{meas}(f_c) + \dots + \phi_{meas}\left(f_c + \frac{N}{2}\Delta_f\right) \quad (7)$$

The experiment was conducted at 1 GHz. First, the reference continuous wave signal radiated by the antenna was measured. Then the LTE signal of different bandwidths was measured using the EMC multiprobe architecture and the parameters at the central frequency extracted. Some comparisons for different bandwidths can be seen in **Figure 11**. The continuous wave (CW) is the reference curve. A deeper analysis of the error pattern can be seen in **Figure 12**. The near-field mean error is very low for both components, below -45 dB. This shows the low error introduced for the field reconstruction.

The correlation between the different signals is very good, demonstrating that the technique used could be suitable to characterize the radiation of EMC devices when modulation is applied. The optimized measurement corresponds to the results

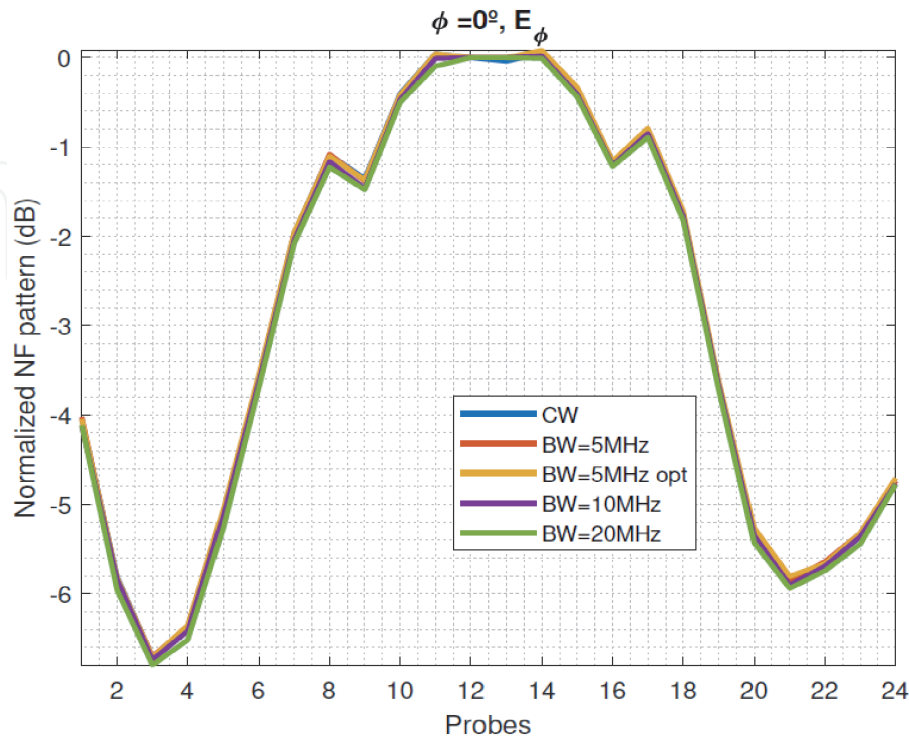


Figure 11. Main cut near-field reconstruction of LTE signal for different bandwidths.

obtained when optimizing the post-processing steps for retrieving the amplitude and phase information of the modulated signal. The same procedure would be applied afterward: near-field to near/far-field transformation at 3 or 10 meters to compare with EMC standards and diagnostics. In this case, the EMC measurement process is explained in **Figure 3**. This test was done on the same PCB used in the previous experiment and was used to validate the performance with a low signal-to-noise ratio, including different signal attenuations, and lower frequencies (400 MHz). Spherical modes are calculated from the acquired near-field, and some spherical mode filtering is applied. This spherical mode filtering consists of canceling those modes that cannot correspond to the signal itself.

The results are shown in **Figure 13**, where the power of the different spherical modes (under m and n index) are shown for the reference case, 30 dB and 65 dB of extra attenuation. It is observed that for 30 dB attenuation, the results are very good, and even for 65 dB attenuation, the results are acceptable. This is also reflected in the right part of **Figure 13**, where the field for different theta angles is shown. Again, the differences are within the typical uncertainty values for EMC setups, even with very low power values, and a frequency lower than the specifications of the multiprobe system for antenna measurements.

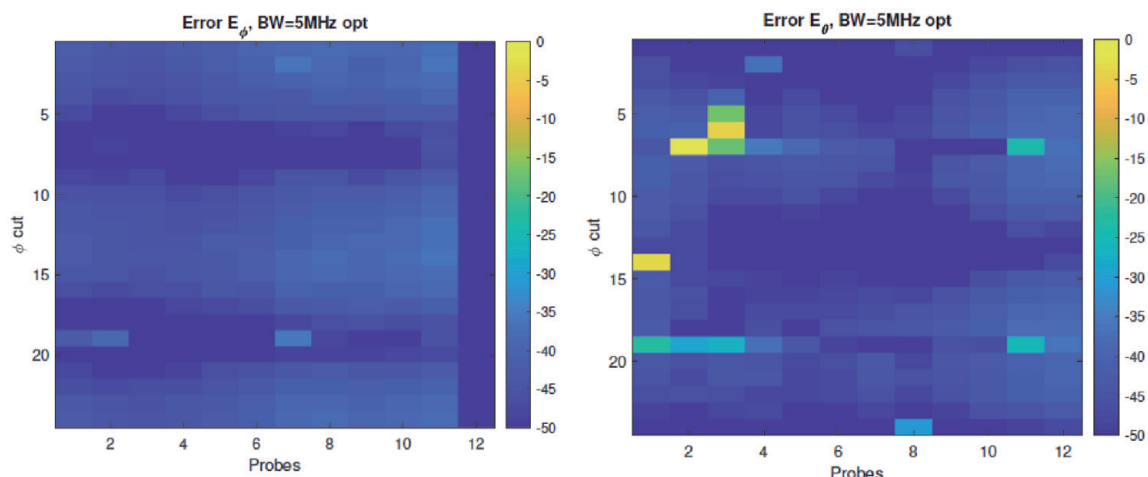


Figure 12. Near-field error between CW signal and EMC multiprobe measurement of 5 MHz LTE FDD signal left (E_ϕ), right (E_θ).

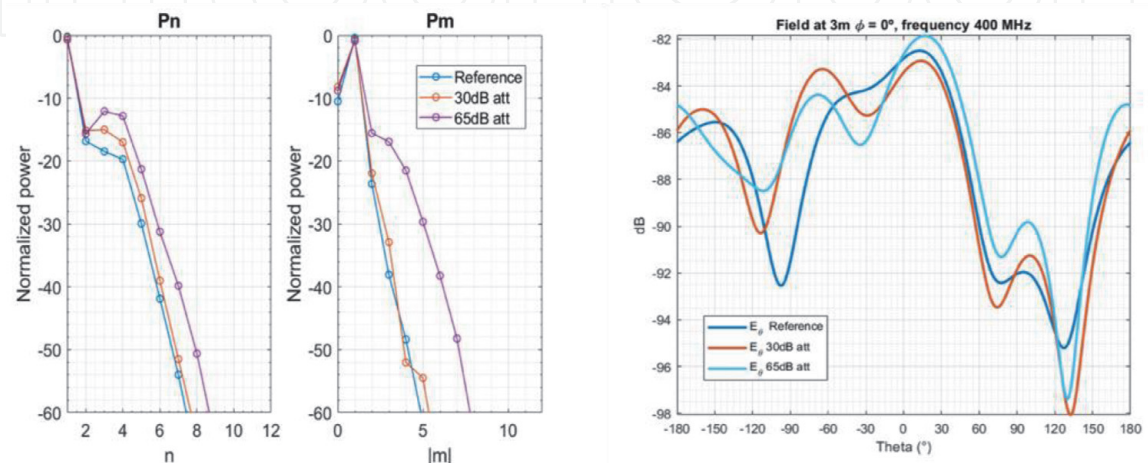


Figure 13. Measurements at 400 MHz, using spherical near-field transformation and mode filtering for different attenuations of the received signal.

These results for EMC multiprobe solution for modulated signals show the potential of this setup, not only for traditional EMC measurements where the spurious emissions are characterized at particular frequencies, but also represents a low cost, accurate and fast solution for addressing pre-compliance of new self-transmitting devices using modulated signals.

7. Conclusions

This chapter has shown the use of antenna measurement techniques to measure the radiation of devices under tests in EMC. The proposed system has been based on the following technologies: multiprobe measurement systems, software-defined radio receivers, phase recovery, spherical near- to far-field transformation software, post-processing techniques as source reconstructions or calculation of equivalent currents and spherical mode filtering, and combination of measurements and simulations.

This process has been validated with measurements in a Microwave Vision Group StarLab system at 400 MHz and 2 GHz, comparing the results with measurements in a conventional EMC setup. The results have shown good agreement, and this is the first step to advance in the use of new technologies of other disciplines, as antenna measurement, to improve the results obtained with the conventional EMC setups.

This chapter has only introduced a summary of the different works done by the authors during the last few years, but most information can be found in some of the references included at the end of the chapter.

Acknowledgements

This work is included in a collaboration between Microwave Vision Group and Universidad Politécnica de Madrid. The Spanish Government also supports it, Ministry of Economy, National Program of Research, Development, and Innovation through the project FUTURE-RADIO “Radio systems and technologies for high capacity terrestrial and satellite communications in a hyperconnected world” (project number TEC2017-85529-C3-1-R).

Conflict of interest

The authors declare no conflict of interest.

IntechOpen

Author details

Rubén Tena Sánchez^{1,2}, Lars Jacob Foged¹ and Manuel Sierra Castañer^{2*}

1 Microwave Vision Group, Pomezia, Rome, Italy

2 Universidad Politécnica de Madrid, ETSI Telecomunicación, Information Processing and Telecommunications Centre, Madrid, Spain

*Address all correspondence to: manuel.sierra@upm.es

IntechOpen

© 2021 The Author(s). Licensee IntechOpen. This chapter is distributed under the terms of the Creative Commons Attribution License (<http://creativecommons.org/licenses/by/3.0>), which permits unrestricted use, distribution, and reproduction in any medium, provided the original work is properly cited. 

References

- [1] Henry W. Ott. *Electromagnetic Compatibility Engineering*. Wiley, 2009. ISBN: 978-0-470-18930-6
- [2] M. Sierra Castañer, Lars J. Foged. "Post-processing techniques in Antenna Measurements." Scitech Publishing (IET). 2019. ISBN: 978-1-78561-537-5.
- [3] Amber Precision Instruments. <http://www.amberpi.com>
- [4] EMSCAN, EMxpert ERX+. "Wideband Very-Near-Field Array of Probes for Efficient EMI Measurements." Presented at COST Action. www.emscan.com
- [5] LUXONDES. <http://www.luxondes.com>
- [6] Batscanner (Nexio Group). <https://nexiogroup.com>
- [7] ICEy. The future of Interference & Compatibility Evaluations. Speag. www.speag.com
- [8] Rubén Tena Sánchez, Manuel Sierra Castañer. "Evaluation of Software Defined Radio Receiver for Phaseless Near-Field Measurements" Proceedings of the 40th Annual Meeting and Symposium of the Antenna Measurement Techniques Association. Williamsburg, Virginia (EEUU), November 4-9, 2018.
- [9] Rubén Tena Sánchez, Manuel Sierra Castañer, L.J. Foged. "Use of Software Defined Radio Receivers for Antenna Measurements." 2019 Photonics & Electromagnetics Research Symposium — Spring (PIERS — SPRING), Rome, Italy, 17–20 June 2019, pp. 1862-1869.
- [10] Rubén Tena Sánchez, Manuel Sierra Castañer, L.J. Foged, D. Gray "EMC Measurement System Based on Software Defined Radio and Diagnostic Techniques" Proceedings of the 41st Annual Meeting and Symposium of the Antenna Measurement Techniques Association. San Diego, California (EEUU), October 6-11, 2019.
- [11] Rubén Tena Sánchez, Manuel Sierra Castañer, L.J. Foged. "Relative Phase Reconstruction Based on Multiprobe Solutions and Post-Processing Techniques." Proceedings of the 14th European Conference on Antennas and Propagation (EuCAP), Copenhagen (Denmark), Virtual Edition May-June 2020.
- [12] Rubén Tena Sánchez, Manuel Sierra Castañer, and L. J. Foged. "A Referenceless Antenna Measurement System Based on Software-Defined Radio" *IEEE Antennas and Propagation Magazine*, Volume: 62, Issue: 5, Oct. 2020. Page(s): 108 – 118. DOI: 10.1109/MAP.2020.3012897
- [13] Rubén Tena Sánchez, Manuel Sierra-Castañer, Ricardo Albarracín-Sánchez, Fernando Rodríguez Varela, Alessandro Scannavini, Lars J. Foged. "Feasibility Study of Near-field Multiprobe System as EMC Measurement Setup". Proceedings of the 15th European Conference on Antennas and Propagation (EuCAP), Düsseldorf (Germany), Virtual Edition 22-26 March, 2021.
- [14] Microwave Vision Group Webpage. <https://www.mvg-world.com/en/products?category=Antenna%20Measurement>
- [15] Rubén Tena Sánchez, Fernando Rodríguez Varela, Lars J. Foged, Manuel Sierra Castañer. "Reconstruction of Relative Phase of Self-Transmitting Devices by Using Multiprobe Solutions and Non-Convex Optimization" *Sensors* 2021, 21, 2459. <https://doi.org/10.3390/s21072459>.
- [16] J. E. Hansen, "Spherical Near-Field Antenna Measurements," London, U.K.: Peter Peregrinus, 1988.

[17] EN 55016-2-3: 2010 Standard. Specification for radio disturbance and immunity measuring apparatus and methods – Part 2-3: Methods of measurement of disturbances and immunity. Radiated disturbance measurements.

[18] UNE-EN 55032:2016 Standard. Electromagnetic compatibility of multimedia equipment - Emission Requirements.

[19] Insight. <https://www.mvg-world.com/es/products/antenna-measurement/software/insight>

[20] StarLab system. <https://www.mvg-world.com/es/products/antenna-measurement/multi-probe-systems/starlab>

[21] MiniLab system. <https://www.mvg-world.com/es/products/antenna-measurement/multi-probe-systems/minilab-6-ghz-ota>

[22] F. Jensen, A. Frandsen, "On the number of Modes in Spherical Wave Expansions." 26th meeting and symposium of the AMTA, Stone Mountain Park, GA, USA, Oct 2004, pp. 489–494.

[23] Catechom. <http://www3.uah.es/catechom/index.php?lang=en>

[24] CST Studio Suite: <https://www.3ds.com/products-services/simulia/products/cst-studio-suite/>

[25] A. P. Mynster and P. T. Jensen, "EMC for the IoT," 2016 International Symposium on Electromagnetic Compatibility - EMC EUROPE, 2016, pp. 144-149